

Investigating the Effectiveness of Explainability Methods in Parkinson’s Detection from Speech

Eleonora Mancini^{*1}, Francesco Paissan^{*2,3}, Paolo Torroni¹, Mirco Ravanelli^{3,4,6}, Cem Subakan^{3,4,5}

¹DISI, University of Bologna, Italy ²Fondazione Bruno Kessler, Italy ³Mila-Québec AI Institute, Canada

⁴Concordia University, Canada ⁵Laval University, Canada ⁶ Université de Montréal, Canada

Abstract—Speech impairments in Parkinson’s disease (PD) provide significant early indicators for diagnosis. While models for speech-based PD detection have shown strong performance, their interpretability remains underexplored. This study systematically evaluates several explainability methods to identify PD-specific speech features, aiming to support the development of accurate, interpretable models for clinical decision-making in PD diagnosis and monitoring. Our methodology involves (i) obtaining attributions and saliency maps using mainstream interpretability techniques, (ii) quantitatively evaluating the faithfulness of these maps and their combinations obtained via union and intersection through a range of established metrics, and (iii) assessing the information conveyed by the saliency maps for PD detection from an auxiliary classifier. Our results reveal that, while explanations are aligned with the classifier, they often fail to provide valuable information for domain experts.

Index Terms—Neural Network Explanations, Interpretable Deep Learning, Parkinson’s Detection

I. INTRODUCTION

Parkinson’s disease (PD) is a progressive neurodegenerative disorder primarily marked by the deterioration of dopaminergic neurons in the midbrain. This degeneration leads to a range of motor and non-motor symptoms, including tremors, bradykinesia, cognitive impairment, and depression [1]–[3]. Importantly, during the prodromal stages of PD, patients often start to exhibit speech impairments, which can serve as early indicators of the disease [4], [5]. Given the non-invasive, cost-effective, and automated nature of speech analysis, researchers have increasingly focused on this approach as a promising avenue for the early detection of Parkinson’s disease [6].

Despite substantial advances in PD classification using speech analysis, model interpretability remains underexplored. In clinical settings, explainable AI (XAI) is essential for providing clear, clinically relevant insights, crucial for the acceptance of automated systems in clinical trials. Many XAI techniques exist for interpreting model predictions, with *post-hoc* explanation methods among the most widely used [7]. Here, we focus on two different sets of approaches: Perturbation-based and Gradient-based *post-hoc* explanation methods. Perturbation-based methods assess feature importance by modifying input data, while gradient-based meth-

ods use gradients of predictions with respect to inputs [8]. Both approaches support local and global explanations, are model-agnostic, and offer valuable insights into the model’s behaviour. This paper systematically evaluates several key perturbation and gradient-based techniques to determine their effectiveness in highlighting PD-relevant speech features, aiming to enhance transparency and clinical utility in PD detection from speech.

Our experimental results show that, although explanations are aligned with the classifier, they often fail to provide insights that are truly informative for domain experts. These methods may lack the level of interpretability required for practical use, emphasizing the need for more effective explainability approaches that connect model behavior with human understanding in specialized domains.

II. RELATED WORK

Various studies have explored automated techniques for identifying speech impairments and using them to predict the progression of Parkinson’s disease. For example, researchers have applied Convolutional Neural Networks (CNNs) on spectrograms of patients’ speech to detect dysarthria, assess its severity and distinguish between PD patients and healthy controls [9], [10]. Some approaches use a combination of one-dimensional and two-dimensional CNNs to capture temporal and frequency information [11], [12]. However, some studies suggest that while these biomarkers are effective, models employing non-interpretable features often outperform those built on more interpretable characteristics [13].

Unfortunately, much of the existing research prioritizes performance metrics over interpretability. As a result, although interpretable speech-based biomarkers have been shown to be useful for Parkinson’s diagnosis [14], little effort has been devoted to comprehensive analysis of explainability in PD detection models. Among the most commonly used XAI methods are perturbation and saliency-based approaches. Some studies employed methods such as GradCAM and EigenCAM to visualize important features. However, these works do not include rigorous quantitative validation of their interpretability. Other approaches, including those using SHAP [15], face challenges in explainability due to the complex input features—such as Mel-frequency cepstral coefficients (MFCCs)—that do not directly correlate with auditory concepts relevant to PD.

In contrast, there has been increasing interest in interpretability for audio and speech applications in recent years.

^{*}Both authors contributed equally to this research. For these authors, the order is alphabetical

This work has been submitted to the IEEE for possible publication. Copyright may be transferred without notice, after which this version may no longer be accessible.

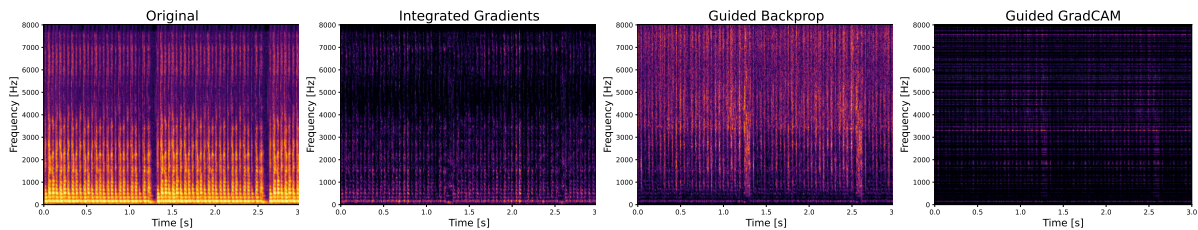


Fig. 1. Explanations generated for a PD sample correctly classified by HuBERT. The explanations highlight different portions of the spectrogram, suggesting that understandability is difficult to achieve in this setting. From left to right: original sample, Integrated Gradients, Guided Backprop, and Guided GradCAM.

Key works have introduced methods like layer-wise relevance propagation [16], masked additive white noise [17], [18], and Guided Backpropagation [19] to understand important spectrogram features. Additionally, SLIME [20], [21] and AudioLIME [22], [23] have explored feature importance within predefined regions of the spectrogram. Recent advancements, such as Listen-to-Interpret (L2I) [24], L-MAC [25], and LMAC-TD [26], have focused on generating listenable explanations in spectrogram and time domains, underscoring the value of interpretability in audio analysis.

In response to the limitations highlighted in PD detection, our work evaluates the effectiveness of XAI methods in the aforementioned context in a systematic way, particularly of perturbation and saliency-based approaches. By comparing various techniques, we aim to provide insights into their effectiveness and limitations, highlighting the potential for explainable AI in clinical applications for Parkinson’s disease.

III. METHODOLOGY

Our methodology to compare and evaluate XAI methods consists of (i) obtaining attributions and saliency maps using mainstream interpretability techniques (Section III-A), (ii) evaluating the explanatory power of such saliency maps (and their combination) quantitatively via a range of metrics defined in the literature (Sections III-B and III-C), and (iii) evaluate the information conveyed by saliency maps for the PD detection task from an auxiliary classifier (Section III-D).

A. Transforming Waveforms for Gradient-Based Attributions

Many SSL-based pre-trained models for audio operate directly on the raw waveform. This is the case also for our PD detection model, HuBERT [27]. In this case, explaining the model predictions in the classifier’s input domain (i.e. on the waveform X_w) results in explanations that are hard to interpret visually. We transform the waveforms into a time-frequency representation X_f using the short-time Fourier transform (STFT). This transformation allows us to compute *attributions* (A) on the spectrogram of the input audio via saliency-based interpretability techniques. Before inputting the audio to the model, we convert the spectrogram back to the time domain using the inverse short-time Fourier transform (ISTFT) and the phase information of the original sample X_w . We apply the following interpretability techniques to generate these maps: Saliency [28], SmoothGrad [29], Integrated Gradients (IG) [30], Guided GradCAM [31], Guided Backpropagation [32], and Guided SHAP [33].

B. Quantitative Analysis through Explainability Metrics

To quantitatively evaluate the quality of the saliency maps, we employ several explainability metrics. Specifically, we adopt metrics previously used in the L-MAC [25], LMAC-ZS [34] and LMAC-TD [26] studies. We use Average Increase (AI), which measures the percentage of samples for which we observe an increase in the classifier’s confidence for the interpretation with respect to the input sample, and Average Decrease (AD), which measures the confidence drop when masking the input with the mask, and Average Gain (AG), similar to AI. Beyond these metrics, we use the Faithfulness (FF) metric defined in the L2I paper [24] and the input fidelity (Fid-In) metric defined in the PIQ paper [35]. We also use the Sparseness (SPS) [36] and Complexity (COMP) [37] metrics to evaluate the conciseness of the explanations. We invite the reader to refer to the cited papers for further details.

C. Exploring Overlap in Explainability Methods

A reasonable expectation when explaining a classifier is that good explanations are aligned with the classifier’s predictions, regardless of the process that generated them. To verify this hypothesis, we investigate the overlap among different attribution methods to assess whether combining them provides further insights into the model’s decisive process. Given a dataset element (X_f, y) , we extract two saliency maps A_1, A_2 using two different explanation techniques (e.g. Saliency and Smoothgrad) and combine them via intersection and union. An increase in explainability metrics through overlapping attributions would suggest that combining methods captures more comprehensive feature representations.

D. Classification Using Saliency Maps and Selective Metrics

Finally, to examine whether the saliency maps derived from each attribution method highlight information pertinent to distinguishing between PD and healthy controls (HC), we train a classifier on the generated explanations. This test is similar to RemOve And Retrain [38]; in our case, however, we measure the amount of information in the explanations in a single iteration. Additionally, we introduce a new set of metrics, called *Selective Metrics*, that scales the standard classification metrics depending on the explanation selectiveness. These metrics penalize explanations replicating the input audio without selectively highlighting the portions of the input relevant to the classification.

To define selective metrics, we combine the classification performance (e.g. accuracy) and the average of the attribution mask. Numerically, for a dataset $\mathcal{D} = \{(X_f, y)_i\}_{i=1}^N$ of N

TABLE I
PD QUANTITATIVE EVALUATION RESULTS OF HUBERT BASE MODEL AVERAGED OVER 10-FOLDS ON S-PC-GITA.

Metric	AI (↑)	AD (↓)	AG (↑)	FF (↑)	Fid-In (↑)	SPS (↑)	COMP (↓)
Saliency	74.66 ± 7.06	1.80 ± 2.22	64.09 ± 13.01	0.004 ± 0.003	82.82 ± 14.27	0.69 ± 0.02	11.98 ± 0.09
Smoothgrad	75.10 ± 8.43	1.85 ± 1.86	55.54 ± 13.42	0.004 ± 0.002	81.89 ± 11.76	0.50 ± 0.02	12.51 ± 0.05
Guided GradCAM	64.99 ± 11.71	5.24 ± 6.74	55.85 ± 16.06	0.001 ± 0.001	82.85 ± 13.83	0.83 ± 0.02	10.69 ± 0.12
Guided Backprop	75.21 ± 6.71	1.62 ± 2.06	64.52 ± 12.90	0.005 ± 0.004	82.67 ± 14.03	0.70 ± 0.02	11.94 ± 0.11
Integrated Gradients	78.83 ± 6.56	1.22 ± 1.72	69.35 ± 9.20	0.013 ± 0.008	81.93 ± 14.32	0.77 ± 0.01	11.69 ± 0.0
Gradient SHAP	76.55 ± 7.59	2.26 ± 3.65	67.46 ± 10.60	0.004 ± 0.003	81.93 ± 13.75	0.69 ± 0.01	11.99 ± 0.06

elements and metric $M(X_f, y)$ (i.e. accuracy, where X_f is the STFT domain input audio), this computes as:

$$S_M(\mathcal{D}) = \frac{1}{N} \sum_{(X_f, y) \in \mathcal{D}} M(X_f, y) (1 - \text{Av}(A)) \quad (1)$$

where $\text{Av}(\cdot)$ denotes the mean that is calculated on the normalized attributions A (which is in $[0, 1]$). This adjustment rewards classifiers that achieve high accuracy while focusing on smaller, relevant input parts. This is particularly relevant to facilitate a comparison between attribution strategies.

IV. EXPERIMENTS

A. Dataset

Standard PC-GITA (s-PC-GITA) is a dataset consisting of recordings from 100 individuals, split evenly between two groups: 50 people with Parkinson’s disease (PD) and 50 healthy controls (HC). Each group includes 25 men and 25 women, with the PD group diagnosed by a neurologist, while the HC group shows no signs of PD or other neurodegenerative conditions. Participants range in age from 31 to 86 years, with recordings captured in a sound-proof booth at Clínica Noel in Medellín, Colombia. The original recordings were sampled at 44.1 kHz with 16-bit resolution and downsampled to 16 kHz for this study, as in [39] and [6]. We use the same splits as those employed by [6] for inference on the test sets of the 10 folds and present the results averaged across these folds; our replicated results, which align with the original paper, are shown in Table II. As in [6], the speech tasks from both datasets considered in this work are diadochokinetic (DDK) exercises, read sentences, and monologues. Additional dataset details are available in [40].

TABLE II
PD RESULTS AVERAGED OVER 10-FOLDS ON S-PC-GITA. MEAN VALUE AND STANDARD DEVIATION ARE REPORTED.

Model	Accuracy	F1-score
HuBERT Base [27]	81.32 ± 8.06	81.03 ± 8.33
WavLM Base [41]	82.10 ± 7.94	81.90 ± 8.09

B. PD Detector

In this study, we build upon recent advancements in the field by relying on a study that explores exploiting foundation models and speech enhancement for Parkinson’s disease detection from speech in real-world operative conditions [6]. In [6], they use SSL models HuBERT [27] and WavLM [41] as foundational backbones for PD detection, extracting high-level representations from raw waveform inputs through a

convolutional and transformer-based encoder. By leveraging pre-trained layers optimized through dynamic weighted summation and an attention pooling head, the model captures discriminative features essential for PD detection, refining these representations with fully connected layers to enhance task-specific accuracy. Following this work, we replicate their results using only the s-PC-GITA datasets and apply explainability techniques to the model.

C. Saliency Maps Classifier

We employ a CNN14 classifier [42] to evaluate saliency maps, taking log-mel spectrograms as input. This classifier is trained for a binary classification task with the following hyperparameters: batch size of 32, learning rate of 0.002, and 50 training epochs.

To train and evaluate the classifier, we construct a dataset from the masks computed on the original test set. For each fold, this dataset is split into training, validation, and test sets with a ratio of 70/15/15, ensuring that the label distribution is stratified to maintain balanced classes across the splits. For comparison, we also train the CNN14 classifier on the original spectrograms from the test set to evaluate performance differences between saliency map-based inputs and the unmodified spectrograms. The CNN14 classifier training is done using the SpeechBrain 1.0 toolkit [43].

V. RESULTS

As shown in Table II, both the HuBERT Base and WavLM Base models obtain comparable results on PD detection. For this reason, we conduct our experiments on HuBERT in this paper. We note that the same experimental protocol and methodology can be applied to interpreting WavLM. Our code is publicly available and can be accessed through our companion website¹, together with additional spectrogram visualizations.

A. Faithfulness Metrics

In Table I, we present the quantitative evaluation results of the HuBERT-base model averaged over 10 folds on s-PC-GITA. We observe that all the XAI approaches show comparable performance overall. The variability in the metrics can be attributed to the high sensitivity of classifier representations to individual subjects, as evidenced by the high standard deviations in Table II. This subject-specific variability leads to fluctuations in faithfulness metrics across folds comparable to those observed on the classification performance. For AI, AD,

¹<https://helemanc.github.io/parkinsons-speech-xai/>

TABLE III
RESULTS OF PD DETECTION USING SALIENCY MAPS.

Metric	Accuracy	Selective Accuracy	F1-score	Selective F1-score	Mask Mean	Mask Std
Saliency	0.87 ± 0.12	0.86 ± 0.10	0.87 ± 0.14	0.85 ± 0.13	0.017	0.037
Smoothgrad	0.86 ± 0.11	0.85 ± 0.11	0.86 ± 0.13	0.85 ± 0.12	0.013	0.020
Guided GradCAM	0.78 ± 0.09	0.78 ± 0.09	0.78 ± 0.10	0.78 ± 0.10	0.002	0.010
Guided Backprop	0.87 ± 0.10	0.86 ± 0.10	0.85 ± 0.14	0.84 ± 0.13	0.016	0.035
Integrated Gradients	0.89 ± 0.08	0.88 ± 0.08	0.89 ± 0.09	0.88 ± 0.09	0.008	0.023
Gradient SHAP	0.84 ± 0.13	0.83 ± 0.13	0.85 ± 0.13	0.84 ± 0.13	0.007	0.019
Original Spectrograms	0.82 ± 0.12	-	0.85 ± 0.10	-	-	-

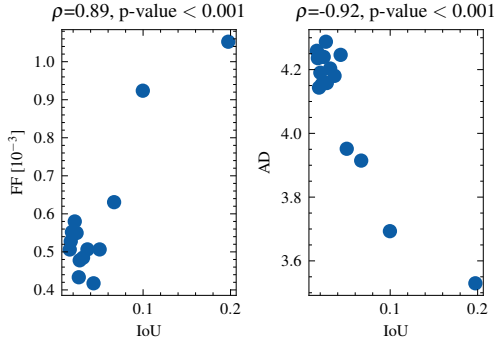


Fig. 2. Analysis of the correlation between explanations overlap among interpretability techniques and faithfulness metrics. Combining interpretability techniques is most effective when there is already significant overlap between attribution masks.

AG, and FF, Integrated Gradients performs best, while for Fid-In, SPS, and COMP, Guided Grad-CAM stands out. This also aligns with the results presented in Table III, in which Guided Grad-CAM shows the lowest mask mean, aligning with its superior performance in SPS and COMP. We note that the small FF values is due to classifier’s uncertainty, since we observed small values in the predicted logit outputs. Overall, we see that the explanations are aligned with the classifier, suggesting that masking the audio spectrogram can be an effective way of highlighting the regions of the input audio associated with the predicted label.

B. Overlap between Explainability Methods

Fig. 2 shows a scatter plot illustrating how faithfulness metrics vary with increasing intersection-over-union (IoU) between explanations from different methods, specifically using intersection as the combination strategy. For the results of the overlap based on the union strategy, we do not observe a linear trend with increasing IoU values. However, we observe that for some metrics (e.g. AD), union is a more effective strategy on average. We focused on two metrics, AD and FF, which showed the most variation across methods. A similar trend is observed on other metrics; we invite the reader to refer to the companion website for the results. Overall, the trend suggests that combining attribution strategies is most effective when the attributions are already well-aligned, supporting our hypothesis that greater mask overlap improves faithfulness metrics.

C. Saliency Maps Classifier

In Table III, we report the classification accuracy and F1-score, together with the corresponding selective metrics. In

most cases, training the classifier on the explanations results in higher classification performance with respect to training on the original data. This suggests that training on the explanations provides better generalization capabilities, possibly because by incorporating explanations, the classifier gains reduced context dependency, thus enhancing its generalization capabilities. Among the XAI methods, Integrated Gradients stands out, excelling in faithfulness metrics and achieving the highest selective accuracy, confirming its overall effectiveness compared to other strategies.

D. Qualitative Analysis

Quantitative results show that explanations align with the classifier outputs and provide helpful information for distinguishing between PD and HC. In Figure 1, we present a sample explanation generated with Guided GradCAM, Integrated Gradients and their combination. In general, we observed that the saliency maps focus on high-frequency regions, potentially reflecting attention to specific phonemes. Nonetheless, these maps are not easily interpretable by humans. We conclude that despite current XAI techniques provide faithful explanations as spectrograms, further research is needed to render explanations more insightful for domain experts. Relevant works in this direction include [44], which relies on additional data modalities.

VI. CONCLUSION

In this paper, we show that popular post-hoc explanation methods can generate faithful explanations for PD detection. Nonetheless, they fail to generate explanations that domain experts can easily understand. We, therefore, suggest that future work should explore approaches that would simplify an input spectrogram such as semantically enriching the spectrogram through phoneme discretization of the spectrogram, creating a direct link between speech biomarkers in PD research and the saliency maps, or investigating methods like listenable explanations (similar to what is proposed in L-MAC) for more intuitive insights.

ACKNOWLEDGMENT

This work was partially supported by project “FAIR - Future Artificial Intelligence Research” – Spoke 8 “Pervasive AI”, under the European Commission’s NextGeneration EU programme, PNRR – M4C2 – Investimento 1.3, Partenariato Esteso (PE00000013).

REFERENCES

- [1] O. Hornykiewicz, "Biochemical aspects of parkinson's disease," *Neurology*, no. 2_suppl_2, pp. S2–S9, 1998.
- [2] W. Poewe, K. Seppi, C. M. Tanner, G. M. Halliday, P. Brundin, J. Volkman, A.-E. Schrag, and A. E. Lang, "Parkinson disease," *Nature reviews Disease primers*, no. 1, pp. 1–21, 2017.
- [3] M. d. De Rijk, L. Launer, K. Berger, M. Breteler, J. Dartigues, M. Baldereschi, L. Fratiglioni, A. Lobo, J. Martinez-Lage, C. Trenkwalder *et al.*, "Prevalence of parkinson's disease in europe: A collaborative study of population-based cohorts. neurologic diseases in the elderly research group." *Neurology*, no. 11 Suppl 5, pp. S21–3, 2000.
- [4] S. Pinto, C. Ozsancak, E. Tripoliti, S. Thobois, P. Limousin-Dowsey, and P. Auzou, "Treatments for dysarthria in parkinson's disease," *The Lancet Neurology*, no. 9, pp. 547–556, 2004.
- [5] J. Ruzs, R. Cmejla, T. Tykalova, H. Ruzickova, J. Klempir, V. Majerova, J. Picmausova, J. Roth, and E. Ruzicka, "Imprecise vowel articulation as a potential early marker of parkinson's disease: effect of speaking task," *The Journal of the Acoustical Society of America*, no. 3, pp. 2171–2181, 2013.
- [6] M. La Quatra, M. F. Turco, T. Svendsen, G. Salvi, J. R. Orozco-Arroyave, and S. M. Siniscalchi, "Exploiting foundation models and speech enhancement for parkinson's disease detection from speech in real-world operative conditions," in *Interspeech 2024*, 2024.
- [7] C. Molnar, *Interpretable Machine Learning*, 2nd ed., 2022.
- [8] M. Mersha, K. Lam, J. Wood, A. K. AlShami, and J. Kalita, "Explainable artificial intelligence: A survey of needs, techniques, applications, and future direction," *Neurocomputing*, 2024.
- [9] B. Sonawane and P. Sharma, "Speech-based solution to parkinson's disease management," *Multimedia Tools and Applications*, no. 19, pp. 29 437–29 451, 2021.
- [10] C. D. Rios-Urrego, S. A. Moreno-Acevedo, E. Nöth, and J. R. Orozco-Arroyave, "End-to-end parkinson's disease detection using a deep convolutional recurrent network," in *International Conference on Text, Speech, and Dialogue*. Springer, 2022, pp. 326–338.
- [11] J. C. Vásquez-Correa, C. D. Rios-Urrego, T. Arias-Vergara, M. Schuster, J. Ruzs, E. Noeth, and J. R. Orozco-Arroyave, "Transfer learning helps to improve the accuracy to classify patients with different speech disorders in different languages," *Pattern Recognition Letters*, pp. 272–279, 2021.
- [12] C. Quan, K. Ren, Z. Luo, Z. Chen, and Y. Ling, "End-to-end deep learning approach for parkinson's disease detection from speech signals," *Biocybernetics and Biomedical Engineering*, no. 2, pp. 556–574, 2022.
- [13] A. Favaro, Y.-T. Tsai, A. Butala, T. Thebaud, J. Villalba, N. Dehak, and L. Moro-Velázquez, "Interpretable speech features vs. dnn embeddings: What to use in the automatic assessment of parkinson's disease in multilingual scenarios," *Computers in Biology and Medicine*, p. 107559, 2023.
- [14] A. Favaro, L. Moro-Velázquez, A. Butala, C. Motley, T. Cao, R. D. Stevens, J. Villalba, and N. Dehak, "Multilingual evaluation of interpretable biomarkers to represent language and speech patterns in parkinson's disease," *Frontiers in Neurology*, 2023.
- [15] M. Maffia, L. Schettino, and V. N. Vitale, "Automatic detection of parkinson's disease with connected speech acoustic features: towards a linguistically interpretable approach," in *Proceedings of the 9th Italian Conference on Computational Linguistics CLiC-it 2023: Venice, Italy, November 30-December 2, 2023*. Accademia University Press.
- [16] S. Becker, J. Vielhaben, M. Ackermann, K.-R. Müller, S. Lapuschkin, and W. Samek, "Audiomnist: Exploring explainable artificial intelligence for audio analysis on a simple benchmark," 2023.
- [17] V. A. Trinh, B. McFee, and M. I. Mandel, "Bubble Cooperative Networks for Identifying Important Speech Cues," in *Proc. Interspeech 2018*, 2018.
- [18] H. S. Kavaki and M. I. Mandel, "Identifying Important Time-Frequency Locations in Continuous Speech Utterances," in *Proc. Interspeech 2020*, 2020.
- [19] H. Muckenhirn, V. Abrol, M. Magimai-Doss, and S. Marcel, "Understanding and Visualizing Raw Waveform-Based CNNs," in *Proc. Interspeech 2019*, 2019, pp. 2345–2349.
- [20] S. Mishra, B. L. Sturm, and S. Dixon, "Local interpretable model-agnostic explanations for music content analysis," in *International Society for Music Information Retrieval Conference*, 2017.
- [21] S. Mishra, E. Benetos, B. L. Sturm, and S. Dixon, "Reliable local explanations for machine listening," 2020.
- [22] V. Haunschmid, E. Manilow, and G. Widmer, "audiolime: Listenable explanations using source separation," 2020.
- [23] S. Chowdhury, V. Praher, and G. Widmer, "Tracing back music emotion predictions to sound sources and intuitive perceptual qualities," 2021.
- [24] J. Parekh, S. Parekh, P. Mozharovskiy, F. d'Alché-Buc, and G. Richard, "Listen to interpret: Post-hoc interpretability for audio networks with nmf," in *Advances in Neural Information Processing Systems*, 2022, pp. 35 270–35 283.
- [25] F. Paissan, M. Ravanelli, and C. Subakan, "Listenable maps for audio classifiers," in *Proceedings of the 41st International Conference on Machine Learning*, 2024, pp. 39 009–39 021.
- [26] E. Mancini, F. Paissan, M. Ravanelli, and C. Subakan, "Lmac-td: Producing time domain explanations for audio classifiers," *arXiv preprint arXiv:2409.08655*, 2024.
- [27] W.-N. Hsu, B. Bolte, Y.-H. H. Tsai, K. Lakhota, R. Salakhutdinov, and A. Mohamed, "Hubert: Self-supervised speech representation learning by masked prediction of hidden units," *IEEE/ACM Trans. Audio, Speech and Lang. Proc.*, 2021.
- [28] K. Simonyan, A. Vedaldi, and A. Zisserman, "Deep inside convolutional networks: Visualising image classification models and saliency maps," 2014.
- [29] D. Smilkov, N. Thorat, B. Kim, F. Viégas, and M. Wattenberg, "Smoothgrad: removing noise by adding noise," 2017.
- [30] M. Sundararajan, A. Taly, and Q. Yan, "Axiomatic attribution for deep networks," in *Proceedings of the 34th International Conference on Machine Learning - Volume 70*, ser. ICML'17. JMLR.org, 2017.
- [31] R. R. Selvaraju, M. Cogswell, A. Das, R. Vedantam, D. Parikh, and D. Batra, "Grad-cam: Visual explanations from deep networks via gradient-based localization," in *2017 IEEE International Conference on Computer Vision (ICCV)*, 2017.
- [32] J. T. Springenberg, A. Dosovitskiy, T. Brox, and M. A. Riedmiller, "Striving for simplicity: The all convolutional net," in *3rd International Conference on Learning Representations, ICLR 2015, San Diego, CA, USA, May 7-9, 2015, Workshop Track Proceedings*, Y. Bengio and Y. LeCun, Eds., 2015.
- [33] S. M. Lundberg and S.-I. Lee, "A unified approach to interpreting model predictions," in *Proceedings of the 31st International Conference on Neural Information Processing Systems*, ser. NIPS'17. Red Hook, NY, USA: Curran Associates Inc., 2017.
- [34] F. Paissan, L. D. Libera, M. Ravanelli, and C. Subakan, "Listenable maps for zero-shot audio classifiers," *arXiv preprint arXiv:2405.17615*, 2024.
- [35] F. Paissan, C. Subakan, and M. Ravanelli, "Posthoc interpretation via quantization," *arXiv preprint arXiv:2303.12659*, 2023.
- [36] P. Chalasani, J. Chen, A. R. Chowdhury, S. Jha, and X. Wu, "Concise explanations of neural networks using adversarial training," 2020.
- [37] U. Bhatt, A. Weller, and J. M. F. Moura, "Evaluating and aggregating feature-based model explanations," 2020.
- [38] S. Hooker, D. Erhan, P.-J. Kindermans, and B. Kim, "A benchmark for interpretability methods in deep neural networks," 2019.
- [39] N. Narendra, B. Schuller, and P. Alku, "The detection of parkinson's disease from speech using voice source information," *IEEE/ACM Transactions on Audio, Speech, and Language Processing*, pp. 1925–1936, 2021.
- [40] J. R. Orozco-Arroyave, J. D. Arias-Londoño, J. F. Vargas-Bonilla, M. C. Gonzalez-Rátiva, and E. Nöth, "New spanish speech corpus database for the analysis of people suffering from parkinson's disease." in *Lrec*, 2014, pp. 342–347.
- [41] S. Chen, C. Wang, Z. Chen, Y. Wu, S. Liu, Z. Chen, J. Li, N. Kanda, T. Yoshioka, X. Xiao, J. Wu, L. Zhou, S. Ren, Y. Qian, Y. Qian, J. Wu, M. Zeng, X. Yu, and F. Wei, "Wavlm: Large-scale self-supervised pre-training for full stack speech processing," *IEEE Journal of Selected Topics in Signal Processing*, 2022.
- [42] Q. Kong, Y. Cao, T. Iqbal, Y. Wang, W. Wang, and M. D. Plumbley, "Panns: Large-scale pretrained audio neural networks for audio pattern recognition," 2020.
- [43] M. Ravanelli, T. Parcollet, A. Moumen, S. de Langen, C. Subakan, P. Plantinga, Y. Wang, P. Mousavi, L. Della Libera, A. Ploujnikov *et al.*, "Open-source conversational ai with speechbrain 1.0," *arXiv preprint arXiv:2407.00463*, 2024.
- [44] S. Gupta, M. Ravanelli, P. Germain, and C. Subakan, "Phoneme discretized saliency maps for explainable detection of ai-generated voice," in *Interspeech 2024*, 2024, pp. 3295–3299.